http://www.jstage.jst.go.jp/browse/biophysics

BIOPHYSICS

Vol. 1, pp. 45–53 (2005)
doi: 10.2142/biophysics.1.45

Fluctuation of actin sliding over myosin thick filaments *in vitro*

Naoki Noda[1], Yasuhiro Imafuku[1], Akira Yamada[2] and Katsuhisa Tawada[1]

[1]*Department of Biology, Graduate School of Sciences, Kyushu University, Fukuoka 812-8581, Japan*
[2]*Kansai Advanced Research Center, National Institute of Information and Communications Technology, Kobe 651-2492, Japan*

Received 17 January, 2005; accepted 8 April, 2005

It is customarily thought that myosin motors act as independent force-generators in both isotonic unloaded shortening as well as isometric contraction of muscle. We tested this assumption regarding unloaded shortening, by analyzing the fluctuation of the actin sliding movement over long native thick filaments from molluscan smooth muscle *in vitro*. This analysis is based on the prediction that the effective diffusion coefficient of actin, a measure of the fluctuation, is proportional to the inverse of the number of myosin motors generating the sliding movement of an actin filament, hence proportional to the inverse of the actin length, when the actions of the motors are stochastic and statistically independent. Contrary to this prediction, we found the effective diffusion coefficient to be virtually independent of, and thus not proportional to, the inverse of the actin length. This result shows that the myosin motors are not independent force-generators when generating the continuous sliding movement of actin *in vitro* and that the sliding motion is a macroscopic manifestation of the cooperative actions of the microscopic ensemble motors.

Key words: protein motors, cooperativity, synchronization

It is customary to consider that myosin II motors are "independent force-generators": the actions of individual myosin heads are stochastic and statistically independent[1]. This idea is derived from previous observations on muscle physiology: (i) the isometric force generated by skeletal muscle is proportional to the overlap between the thick and thin filaments in the sarcomere[2] and (ii) reducing the overlap in the sarcomere has virtually no effect on the steady-state speed of the isotonic shortening of skeletal muscle under a very light load[3]. However, these observations are not sufficient to conclude that myosin II motors are independent force generators. Analyses on the system-size dependence of fluctuations in the context of mathematical statistics (= the central limit theorem[4]) are necessary.

Fluctuation analyses are practically impossible with muscle fibers because there are too many myosin molecules present in even a tiny single fiber. In contrast, using the motility or force assay method *in vitro*, such analyses are feasible owing to the relatively small number of myosin molecules involved in the assay. Ishijima et al.[5] thus studied the fluctuation of the isometric force generated *in vitro*. They found that the relative force fluctuation is proportional to $1/\sqrt{N}$, where N is the number of myosin heads interacting with an actin filament. Their finding is consistent with the mathematical-statistical manifestation based on the view that myosin heads independently generate isometric force.

The assumption of the independent action of myosin II heads driving the unloaded sliding movement of an actin filament can be tested by another fluctuation analysis of the movement observed using the *in vitro* motility assay, movement which is an *in vitro* correlate of the unloaded shortening of muscle[6]. This is the issue we address in this study. The fluctuation analysis we herein employed is based on the prediction that the variance of the sliding distance of an actin filament for a given time interval is proportional to the inverse of the number of myosin motors generating the actin sliding motion, hence proportional to the inverse of the actin length, if myosin motors are independent force-generators[7].

Corresponding author: Katsuhisa Tawada, Department of Biology, Graduate School of Sciences, Kyushu University, Fukuoka 812-8581, Japan. e-mail: ktawascb@mbox.nc.kyushu-u.ac.jp

This is another manifestation of the central limit theorem applied to a filament driven to slide by myosin motors in an ensemble.

In the conventional *in vitro* motility assay, the orientations of motor proteins are random. Their random orientations may impede the interpretation of the results with such *in vitro* motility assays in the context of mathematical statistics[8]. In this work, therefore, we studied actin sliding over myosin thick filaments, from which myosin motors are naturally oriented. Herein we used native myosin thick filaments taken from molluscan smooth muscle[9,10], which are straight and long (20~50 μm), and hence are more suitable for our fluctuation analysis of actin sliding.

Our findings show that the effective diffusion coefficient of the actin filament, which is obtained from the variance of the actin sliding distance as a function of the time interval, is virtually independent of the actin filament length, contrary to the above prediction. This length independence therefore indicates that myosin motors are not "independent force-generators" when they are generating the unloaded continuous sliding of an actin filament *in vitro*. One possible explanation for our results is to assume that the ensemble myosin molecules which generate the continuous sliding motion of an actin filament act synchronously.

Materials and methods

Proteins

Actin was purified from an acetone powder of rabbit skeletal muscles according to Spudich & Watt[11] and was polymerized in the presence of a slight molar excess of rhodamine-phalloidin. Native thick filaments were isolated, as described previously[12], from the anterior byssus retractor muscle (ABRM) of the bivalves *S. virgatus* and *M. gallo-provincialis*, all collected at nearby seashores.

Motility assay *in vitro*

We observed the movement of fluorescent actin filaments over thick filaments, using the protocols of Yamada & Takahashi[13]. In brief, isolated thick filaments were introduced into a flow cell made of coverslips so that they could attach themselves to the glass surface. A solution of actin filaments (2.7 nM in monomeric form) labeled with rhodamine-phalloidin in motility buffer (71 mM KCl, 2.1 mM $CaCl_2$, 2.8 mM $MgCl_2$, 1.9 mM EGTA, 0.9 mM ATP, 9.4 mM DTT, 9.4 mM PIPES buffer (pH 7.0), 3.8 mg/ml glucose, 7.5 μg/ml catalase, and 38 μg/ml glucose oxidase) was then infused into the flow cell. Thick filaments fixed on the glass surface and actin filaments sliding over them were respectively visualized under dark-field illumination and epi-fluorescence illumination, using a Zeiss AXIOVERT 200 inverted microscope equipped with a Plan-APOCHROMAT ×100 objective lens (N.A.=1.4), a Zeiss dark-field condenser (N.A.=1.2–1.4) and a high sensitivity SIT television camera (C2400-08, Hamamatsu Photonics, Hamamatsu, Japan). First, the images of dark-field illuminated thick filaments, and then, the images of fluorescent actin filaments sliding over the thick filaments, were recorded using a Hi8 mm videocassette recorder (EVO-9650, SONY, Tokyo, Japan). All experiments were performed at 25°C.

Data collection

Video images of fluorescent actin filaments were transferred to a computer frame by frame, and the (x, y) coordinates of their front tips in each frame were digitized by using a mouse-driven cursor on the screen. The positional data were then processed with a computer, as described previously[14]. Since native thick filaments are bipolar[9,10], care was taken so as to determine the positions of a sliding actin filament while its entire length stayed within the range of a half side of a thick filament. In this study, the movements of actin filaments sliding toward the center of thick filaments were analyzed. The sampling interval for the positional determination was 1/30 sec. Usually more than 100 positional data points were obtained from a single trajectory of actin sliding movement. The tape recorder, image digitization and image processing were all controlled by a customized software package. The magnification was 136 nm/pixel and 126 nm/pixel for the x- and y-axes, respectively.

Positional trajectories of sliding actin filaments

The positional trajectory of each actin filament was fitted with either a straight line or a polynomial curve by least square regression, and each position was projected perpendicularly onto the fitted line or curve, to eliminate any lateral components (= residuals) of the actin displacements[15]. We usually assessed each fit by inspecting a scatter plot of the residuals. When a scatter plot of the fitting has a random appearance, we regard the fit as a good one. Although polynomial curve fitting worked better than straight line fitting based on this criterion of the scatter plots, we found that the straight line and polynomial curve fittings gave practically the same results for the purpose of our present study, and hence only the results obtained with the straight line fitting are shown in the Results.

Data analysis

The variance of the actin sliding displacement was evaluated by

$$\sigma_r^2 = <(r(\Delta t) - <r(\Delta t)>)^2> = 2D_m\Delta t + \sigma_{r0}^2 \quad (1)$$

where $r(\Delta t)$ is the net displacement of an actin filament along its trajectory in a given time interval (Δt), $<\cdot>$ shows the average, D_m is the effective diffusion coefficient, and σ_{r0}^2 is a term due to position measurement errors[14,16]. The values of $r(\Delta t)$ for the average calculations in Eq. 1 were obtained by calculating the contour lengths between pairs of positional points projected on a trajectory line for a given time interval Δt[14,17], as follows. A single trajectory of actin move-

ment consists of a series of n positional points (p(i), i=0 ... n−1). A set of the net displacements $r(\Delta t)_0$, $r(\Delta t)_1$, $r(\Delta t)_2$, ..., for $\Delta t = j \times \tau$ (j=1, 2, ..., n−1), are given by $r(\Delta t)_i = p(t_i+\Delta t) - p(t_i)$ where i=0, 1, ..., (n−1−j) and τ is the data acquisition time interval (=1/30 sec). Note that the net displacements thus obtained from a single trajectory consist of some overlapping data components. Alternatively, net displacements can be obtained from a single trajectory without any overlapped components. Net displacements obtained with the non-overlap method have a smaller number of data than those obtained with the overlap method. If non-overlap net displacements are used for the average calculation of Eq. 1, then the scatter is hence larger and the determination of D_m is more difficult, as shown by the simulation in the Supplementary Materials. As is also shown by the simulation in the Supplementary Materials, the overlap method does not affect the determination of D_m. As a result, we used the overlap method in this study. The single trajectory averaging thus yields a value of D_m for individual sliding actin filaments of various lengths. The average sliding velocity (V) was evaluated by the slope of a straight regression line between r(Δt) and Δt for the trajectory of each actin filament.

In the present study, we measured the position of an actin filament at its front tip as described above. In the original development of the method employed here for the actin movement analysis, however, the position of an actin filament was given by that of the 'center of mass' of the filament[7], not by that of its front (or rear) tip. Position measurements of actin filaments at their tips yield the same values for D_m in Eq. 1 as do those at their center of mass, since actin filaments in our motility assay system can be considered to be longitudinally rigid, as shown below.

Suppose an actin filament is sliding linearly over a myosin filament. We denote the positions of its front tip and its center of mass at time t by F(t) and C(t) respectively, and the length between the front tip and the center of mass by LM(t). The net displacement of the filament in a given time interval (Δt), $\Lambda_c(\Delta t)$, is given by $\Lambda_c(\Delta t) = C(t+\Delta t) - C(t)$, if the position of the center of mass of the filament is used. A set of the net displacements $\Lambda_c(\Delta t)$'s, which can be obtained from a discrete time series equi-temporally constructed from a single trajectory of an actin filament C(t), yields a value for D_m by

$$<(\Lambda_c(\Delta t) - <\Lambda_c(\Delta t)>)^2> = 2D_m\Delta t. \quad (2)$$

When the positions of the center of mass of an actin filament are digitized on a pixel lattice of the screen, digitization errors are introduced into the coordinates of the positions. In this case, we have

$$<(\Lambda_{cd}(\Delta t) - <\Lambda_{cd}(\Delta t)>)^2> = 2D_m\Delta t + 2\varepsilon_d^2, \quad (3)$$

where $\Lambda_{cd}(\Delta t)$ is the net displacement of actin in Δt obtained from the digitized positional data of the center of mass and ε_d is the standard deviation of the digitization errors. The factor of 2 in front of ε_d^2 comes from the fact that both ends of a displacement length $\Lambda_{cd}(\Delta t)$ are subjected to digitization errors[18]. The magnitude of $\sqrt{2} \times \varepsilon_d$ is close to the pixel-pixel unit distance (about 130 nm).

If the front tip position is used, the net displacement, $\Lambda_f(\Delta t)$, is given by $\Lambda_f(\Delta) = F(t+\Delta t) - F(t)$. Since $F(t+\Delta t) = C(t+\Delta t) + LM(t+\Delta t)$ and $F(t) = C(t) + LM(t)$, we have $\Lambda_f(\Delta t) = \Lambda_c(\Delta t) + \zeta$, where ζ (=LM(t+Δt)−LM(t)) shows length fluctuations of actin due to its compliance during sliding movement. The actin thin filament during isometric contraction of muscle is stretched by 0.2 to 0.35%[19,20]. However, the thin filament length does not change appreciably in muscle shortening under a near-zero load[21]. The shortening of muscle under this condition is a correlate of the actin sliding over myosin filaments *in vitro* in our motility assay. Even if we assume that actin filaments are stretched or compressed by 0.02 to 0.035% (=10% of the length change of the thin filament during muscle isometric contraction) in our motility system, $|\zeta|$ for a 10 μm actin filament must be less than 2 nm, which is negligibly small as compared with the magnitude of positional digitization errors. Therefore, we can suppose that actin filaments are not stretched or compressed (= longitudinally rigid) in our actin motility assay system, and that $\zeta = 0$. We thus have $\Lambda_f(\Delta t) = \Lambda_c(\Delta t)$ and consequently have the same value for D_m with the positional measurements at the actin front tip as with those at the center of mass. When the positions of the front tip of an actin filament are digitized on a pixel lattice, they result in the following equation:

$$<(\Lambda_{fd}(\Delta t) - <\Lambda_{fd}(\Delta t)>)^2> = 2D_m\Delta t + 2\varepsilon_d^2, \quad (4)$$

where $\Lambda_{fd}(\Delta t)$ is the net displacement of actin in Δt obtained from the digitized positional data of the actin front tip and ε_d is the standard deviation of the digitization errors. Since $\Lambda_{fd}(\Delta t)$ corresponds to r(Δt) in Eq. 1, a comparison of Eq. 1 with Eq. 4 reveals that the term σ_{r0}^2 in Eq. 1 must have a value close to that of $2\varepsilon_d^2$ if positional measurement errors are mostly due to positional digitization on a pixel lattice.

Results

1/length dependence and simulation

In this work, we analyzed the sliding movement of single actin filaments driven by the myosin heads. Actin sliding movements include intrinsic fluctuations owing to the myosin-actin interactions. As a result, the variance of the actin sliding displacements grows over time (see Eq. 1). The relationship between the variance and time yields an effective diffusion coefficient (D_m) (see Eq. 1). The effective diffusion coefficient of an actin filament is thus a measure of the fluctuation inherent in the actin sliding displacements.

The longer the actin filament, the larger the number of myosin heads involved in the interaction with the actin filament. Consequently, if the actions of individual myosin heads which cause an actin filament to slide are stochastic and statistically independent, then the fluctuation in the

actin sliding displacements generated by the ensemble heads for a given time interval is smaller, owing to the attenuation of the actions of individual myosin heads by more myosin-actin interactions in longer actin filaments. Since the number of myosin heads driving an actin filament to slide is proportional to the actin length under the above 'independent actions' assumption, the effective diffusion coefficient is thus proportional to the inverse of the actin filament length[7], as is the diffusion coefficient (D) of a filamentous particle undergoing a Brownian movement along its long axis to the inverse of the filament length[22]. The same 1/length dependence of the diffusion coefficient has also been found with microtubules in their Brownian movements generated by enzymatically inactive dynein and mutant ncd motors[23–25]. The 1/length dependence of D_m and D is a direct consequence of the mathematical statistics based on the premise that the actions of either protein motors or solvent molecules are stochastic and statistically independent[4]. To gain a better understanding of the 1/length dependence of D_m, we performed a computer simulation, although the 1/length dependence is model-independent as shown theoretically[7]. For the simulation, we use a simple model following Huxley's 1957 model[26]. The simulation model considers the sliding of an actin filament generated by an ensemble of myosin motors. In the model, 'spring' myosin units are distributed in a relatively long array, and myosin-binding sites are discretely distributed on an actin filament of a given length (Fig. 1, inset). We herein consider, for the first time, the uniform distribution of myosin units. We assume that the actions of individual myosin heads, i.e., attachment and detachment of myosin units to and from actin, are stochastic and statistically independent. The attachment and detachment rates are assumed to depend on the distance between a myosin unit and the nearest binding site on actin as shown in Huxley's 1957 model[26] (Fig. 1, inset).

We performed Monte Carlo simulations of the model shown in the inset of Fig. 1 with the above assumptions (see the Supplementary Materials for details), and collected data on the sliding displacements of the actin filaments with various lengths for various time intervals. From the displacement data we evaluated the effective diffusion coefficient for each actin filament using Eq. 1. The effective diffusion coefficients (D_m) are plotted against the actin length in Fig. 1, which shows an inverse relationship between the effective diffusion coefficient of actin and the actin length. The inverse relationship under the random action assumption of myosin units was confirmed by simulations under various conditions including the heterogeneous distribution of myosin units as well as by simulations of two different models (see Supplementary Materials for details).

Fluctuation in the actin sliding movement *in vitro*

Fig. 2A shows an example of the original positional trajectory of an actin filament sliding over a native thick filament isolated from a single bivalve animal. To eliminate

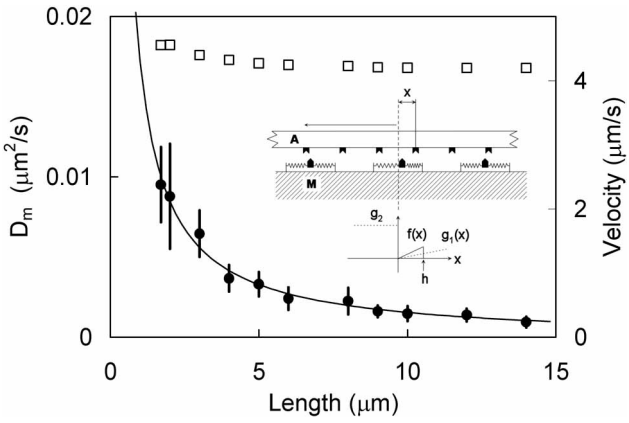

Figure 1 Effective diffusion coefficient (D_m, filled circles) and average sliding velocity (open squares) versus the actin length in a Monte Carlo simulation. The D_m values in the figure are the mean±SD (for N=10 different simulation runs). The filled curve represents β/(actin length) fitted to the D_m data by non-linear regression, where β=0.0173 μm^3/s. If the D_m data were plotted against 1/(actin length) rather than the actin length, the plot could be fitted to a linear line passing through the origin, indicating that D_m approaches zero with the infinite increase in the actin length. The sliding velocity is virtually independent of the actin length above a certain length (>3 μm). Inset, a model of actin (A) sliding over an ensemble of myosin (M) units; x: the distance between a myosin unit and the myosin-binding site on actin; f(x): attachment rate; g_1(x) and g_2: detachment rates; h=10 nm. Under the standard conditions in the present simulation, f(h)=43.33 s^{-1}, g_1(h)=10 s^{-1} and g_2=836 s^{-1}; the separation between the nearby two sites on actin=5.5 nm and that between the nearby two myosin units=42.9 nm.

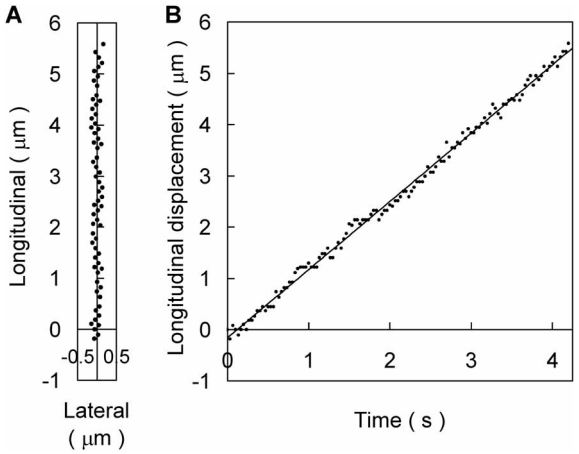

Figure 2 An example of the movement of an actin filament over a native thick filament from the molluscan smooth muscle. The lengths of the actin filament and the myosin filament were 1.8 and 48.1 μm respectively. A, Trajectory (127 positional data points) of the front tip of the actin filament in the x-y plane. The filled circles show the tip position in each video frame. The center perpendicular line is a linear regression line applied to the original data points. B, Positions of the actin tip projected onto the linear regression line in A, the longitudinal components, as a function of time. The filled line is a linear regression line applied to the longitudinal components. The slope of the line yields a value of 1.33 μm/s for the average sliding velocity.

any minor lateral components of the actin displacements, the trajectory was fitted to a straight line (Fig. 2A), and each position was projected perpendicularly onto the fitted line. The scatter of the lateral components appears almost random (Fig. 2A), thus indicating a satisfactory fitting. The distribution of the lateral components fits a Gaussian distribution with a standard deviation ($=\sigma_{lc}$) of 71 nm and the mean=0 (see Supplementary Figure 1A). This indicates that 95% of the lateral components fall within $\pm 2\sigma_{lc}$ (=142 nm, approximately equal to the pixel-pixel unit distances). Therefore, the lateral components represent mostly the uncertainties of the position measurements due to digitization. The lateral components did not depend on the actin length (see Supplementary Figure 1B). This result together with the fact that the actin trajectory was fitted to a straight line indicates that actin did not wobble during its sliding movement within the accuracy of positional measurements in the present experiments. Fig. 2B shows the longitudinal displacement after the adjustments as a function of time. The slope of the fitted regression line in Fig. 2B yields a value of 1.33 μm/s for the average sliding velocity.

The variance in the sliding displacements of an actin filament for various given time intervals was obtained by a single trajectory averaging with Eq. 1 (see Materials and methods). The variance is plotted against the time interval in Fig. 3, thus showing that the variance grew over time. This time-dependent term is due to the fluctuation inherent in the sliding motion rather than artifactual noises (see Imafuku et al. for further clarification[14,16]).

The half of the slope of the fitted regression line in Fig. 3 yields a value of 0.012 $\mu m^2/s$ for D_m in Eq. 1. We obtained the linear line, using a linear regression method similar to that used by Uyeda et al.[15], as follows. A series of straight lines were fitted to initial portions of this variance-time interval curve, each passing through the first two data points (those at $\Delta t=\tau$ and 2τ), the first three data points (those at $\Delta t=\tau$, 2τ and 3τ),…, the first N data points (those at $\Delta t=\tau$, 2τ, ..., and $N\tau$), where τ is the data acquisition time interval (=1/30 sec). With each linear line fitted to the first N data points, the square deviation of the variance (vertical-axis) value from the fitted line was scored for all the N data points used for the regression and summed. The sum was divided by N, yielding the average ($<\delta^2>$). The average square deviation together with the slope of the regression line is shown as a function of N (or as a function of the corresponding time interval) in the inset in Fig. 3. With the increase in the number N, the average square deviation $<\delta^2>$ increases and temporarily reaches a steady level (with occasional minor 'bumps'), and the slope of the line initially fluctuates and then maintains a relatively constant value. With further increase in the number N, the slope begins to change. The average square deviation $<\delta^2>$ often concomitantly begins to grow rapidly. As shown by computer simulation (see Supplementary Materials), the number N_c, right before the line slope begins to change and $<\delta^2>$ most often

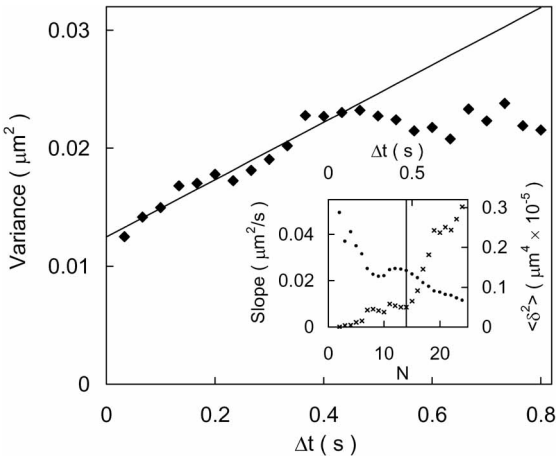

Figure 3 Variance of the actin sliding distance as a function of the time interval. The variance was calculated by averaging within the single linear trajectory shown in Fig. 2B. The filled line indicates an appropriate, initial linear portion of the curve of the data points (filled diamonds) for the determination of a D_m value by Eq. 1 (in Materials and methods). See the text for the method used to identify the appropriate, initial linear portion, and also for the Inset figure (filled circles: slope, crosses: $<\delta^2>$).

concomitantly begins to grow rapidly, provides the number of the best initial data points for identifying an initial linear portion in the variance-time interval curve to estimate the effective diffusion coefficient. In the case shown in this inset, the N_c was 14.

In some cases a clear flat portion followed by an abrupt increase of $<\delta^2>$ can not be identified in a plot shown in this inset. Such trajectories were rejected and not used for further analyses (see Supplementary Materials). Based on this criterion, 41% of the total trajectory data were rejected in this study. The fraction of the rejected data did not depend on the actin length (see Supplementary Figure 2). About 40% of trajectories (each trajectory consisting of 127 positional data points, the same number as that in Fig. 2A) generated by computer simulations using two different models was found to be the type of trajectory that was unable to be used for estimating D_m with the method shown in the inset in Fig. 3 (see Supplementary Materials). The fraction of this type of trajectory was found to be smaller if the number of positional data points in a single trajectory was much larger in computer simulations. When the number of positional data points was 1000, for example, there was no such trajectory (see Supplementary Materials).

The downward deviation from linearity after a certain time interval (>0.47 sec in Fig. 3) represents an artifact introduced by the overlap method used in single trajectory averaging, *i.e.* this is caused by an increase in the representation of overlapping data when long time intervals are used (see Supplementary Materials; Imafuku et al.[14]). The time duration before the downward deviation from linearity varies from experiment to experiment even when tracks have the same number of positional data points, and the

initial linear portion is longer if the number of positional data points is larger, as shown by simulation (see Supplementary Materials). The position measurement errors do not accumulate over time, unlike the fluctuation inherent in the sliding motion, and contribute as a constant value in the variance of sliding displacement ($=\sigma_{r0}^2$ in Eq. 1). The intercept on the ordinate of the regression line in Fig. 3 hence yields a value of 112 nm for σ_{r0}, an estimate for the position measurement errors along the translational direction[14,16]. The values of σ_{r0}^2 did not depend on the actin length (see Supplementary Figure 3).

As shown above, the lateral components are mostly positional digitization errors. In measuring the lateral components (Fig. 2A), one end of a lateral component line is subjected to the measurement errors due to position digitization, whereas the other end of the line is not because the coordinates of the latter end are given by a regression line. Unlike in the lateral components, both ends of a sliding displacement line are subjected to position measurement errors due to digitization. If we assume that the measurement error σ_{r0}^2 mostly originates from the digitization as do the lateral components, hence, the time-independent term in the variance of the sliding displacements, σ_{r0}^2, must be two times larger than the variance of the lateral components ($=\sigma_{lc}^2$)[18]. This relationship, in other words $\sigma_{r0}=\sqrt{2}\sigma_{lc}$, is consistent with a set of the values obtained above (112 nm for $\sigma_{r0}\approx\sqrt{2}\times71$ nm for σ_{lc}) as well as a set of the average values obtained with 39 different actin trajectories (122 nm for $\sigma_{r0}\approx\sqrt{2}\times78$ nm for σ_{lc}). This consistency substantiates that the time-independent term in the variance of the sliding distances originates mostly from the uncertainties of the position measurements due to digitization as do the lateral components.

Length Independence of D_m

Likewise, we repeated the fluctuation analysis with thick filaments (8 in total) isolated from the same animal of *S. virgatus* used for the analysis shown in Figs. 2 and 3, to evaluate the effective diffusion coefficients of individual actin filaments sliding over the myosin filaments. The effective diffusion coefficients thus evaluated are plotted against the actin filament length in Fig. 4A (filled circles). The open squares in this figure show another example of the results from the same analysis, which was carried out with myosin filaments isolated from an animal of another species, *M. galloprovincialis*. As shown in Fig. 4A, the effective diffusion coefficient of actin filaments is not proportional to 1/(actin length); the coefficient does not appreciably depend on the actin length in both bivalves. This is in sharp contrast to the prediction of the inverse length dependence derived from the assumption of the stochastic and statistically random actions of myosin motors.

The sliding velocity of actin filaments over each of the myosin filaments of the two different bivalves did not depend on the actin length in the range we studied (Fig. 4B).

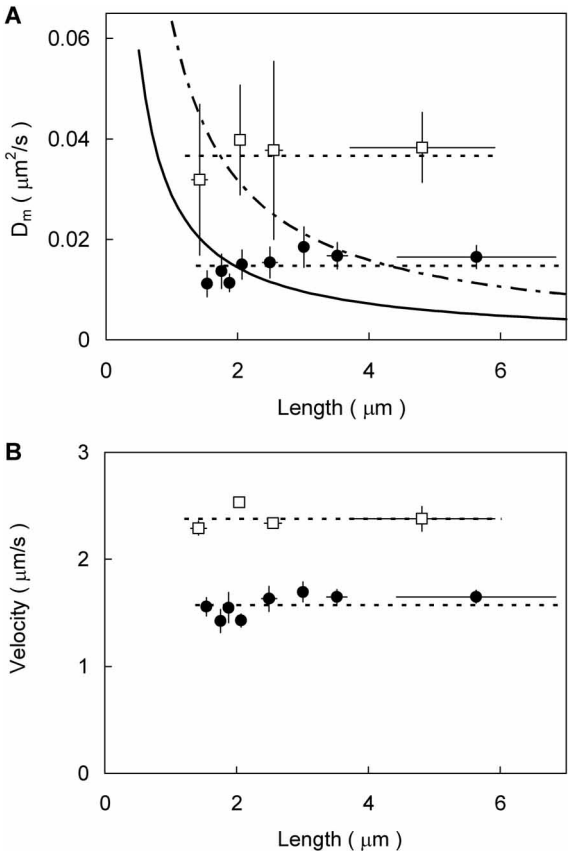

Figure 4 Examples of the effective diffusion coefficient (D_m) (A) and the sliding velocity (B) as a function of the actin length. Open squares, Data were collected with 17 different actin filaments (1.1~8.0 μm) sliding over 8 different single thick filaments (16.6~30.1 μm) isolated from an animal of *M. galloprovincialis*. The data points from the left show the average taken over the effective diffusion coefficients (A) or the sliding velocities (B) for N=5, 4, 4, and 4 different actin filaments. Filled circles, Data were collected with 39 different actin filaments (1.3~9.2 μm) sliding over 8 different single thick filaments (40.5~54.0 μm) isolated from an animal of *S. virgatus*. The data points from the left represent the average taken over the effective diffusion coefficients (A) or sliding velocities (B) for N=5, 5, 5, 5, 5, 5 and 4 different actin filaments. The ordinate and abscissa in both panels are mean±s.e.m. Broken lines show the averages: those of D_m and velocity are 0.037 (open squares) and 0.015 (filled circles) μm²/s in A, and 2.4 (open squares) and 1.6 (filled circles) μm/s in B, respectively. Dotted-dash and solid lines in A are curves of 1/(actin length) fitted by non-linear regression either to the D_m values of *M. galloprovincialis* or to those of *S. virgatus*, respectively . These lines were fitted to individual D_m values before binning.

The length independence of the actin sliding velocity is consistent with findings previously obtained with conventional *in vitro* motility assays with myosins randomly dispersed on a solid surface[27,28]. The sliding movement of actin filaments shorter than about 1 μm was found to be slower (data not shown). The slower sliding of such short actin filaments is a result of their temporary detachment from myosin heads[29]. Since temporarily detached actin filaments are subjected to thermally-agitated Brownian motion, their effective diffusion coefficients are expected to have an additional 1/length-

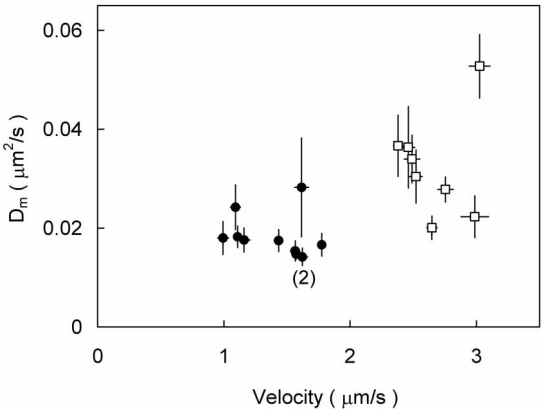

Figure 5 Correlation between the effective diffusion coefficient and the sliding velocity. Each point represents a data set (mean±s.e.m.) obtained with a separate animal of either *M. galloprovincialis* (open squares) or *S. virgatus* (filled circles). There are two data points at (Velocity=1.6, D_m=0.015), which is marked by (2) in the panel. Assuming a linear correlation between the x- and y-axes, we obtained 0.60 for the linear-correlation coefficient *r*. The probability that a random sample of Ns (=18) uncorrelated experimental data points would yield an experimental linear-correlation coefficient as large as or larger than the observed value of $|r|$ was calculated from the equation of Bevington & Robinson[18], and the result was <0.85%. This small value indicates that D_m and the velocity are unlikely to be uncorrelated.

dependent term[14]. Note that the 1/length-dependent term diminishes, as the length is large enough. In this study, therefore, we analyzed the effective diffusion coefficient of actin filaments longer than about 1 μm, where the velocity did not depend on the actin length.

Correlation between D_m and the average sliding velocity

We confirmed the length-independence of both the sliding velocity and effective diffusion coefficient of actin filaments, using myosin filaments isolated from 16 additional different animals (9 animals of a bivalve species, *S. virgatus,* and 7 animals of another bivalve species, *M. galloprovincialis*) (data not shown). The sliding velocity of actin filaments over myosin filaments isolated from *M. galloprovincialis* is faster than that over myosin filaments isolated from *S. virgatus*, and the effective diffusion coefficient of actin filaments over the former myosin filaments is correspondingly larger than that over the latter myosin filaments on the average (compare the data points shown by the open square marks and those shown by the filled circle marks in Fig. 5). Although the sliding velocity of the actin filaments over different myosin filaments isolated from a single animal of a bivalve species appears to be almost the same (see the small error bars for the velocity of each point in Fig. 5), the actin sliding velocity over myosin filaments varied to some extent from animal to animal even within each species of the bivalve, and the effective diffusion coefficient also varied. There thus appears to be a positive correlation between the effective diffusion coefficient and the sliding velocity of actin filaments (Fig. 5).

Discussion

In this study, we found that the effective diffusion coefficient (D_m) of actin filaments sliding over native myosin thick filaments is virtually independent of the actin length (Fig. 4A). This is contrary to the prediction of 1/length dependence, which is derived from the assumption that myosin II is an independent force generator when generating unloaded actin sliding movement. Therefore, the length independence of D_m shows that myosin II is not an independent force generator; the actions of myosin II molecules in an ensemble driving an actin filament to slide are not stochastic and statistically independent. This in turn indicates the presence of cooperativity or synchronization in the myosin actions generating the actin sliding movement *in vitro*. This contrasts sharply with the conclusion in the isometric condition study *in vitro* reached by Ishijima et al.[5] They analyzed the fluctuations of tension by using a stiff fine needle with its tip attached to one end of an actin filament placed over myosin motors under the isometric condition, where there was no translational sliding movement between actin and myosin, and concluded that actions of myosin heads are random based on the central limit theorem[5].

The fluctuation analysis of the sliding distance we employed in this paper can be applied to the loaded sliding movements of actin filaments as well as their unloaded sliding movements. This has been demonstrated by our computer simulation study that used the Duke model of muscle contraction[30]. His model indicates that (i) myosin motors in an ensemble are synchronized in muscle shortening only within a limited range under a relative load (~0.7) and (ii) the motors are not synchronized in the other ranges of the relative load or in isotonic unloaded shortening muscle. Our computer simulation study of actin sliding movements based on his model has demonstrated that (a) the effective diffusion coefficient of actin filaments is length-independent in the range of the relative load where the Duke model predicts synchronization of ensemble myosin motors, and (b) the effective diffusion coefficient is proportional to 1/length in the other ranges of the relative load including the unloaded condition (Imafuku et al., manuscript in preparation). It should be noted that the indication (ii) of the Duke model for the case of the unloaded shortening and the corresponding result (b) of the computer simulation are not consistent with the experimental results we presented in this paper.

Recently, Liu & Pollack[31] reported that sliding between an isolated actin and a myosin filament at a relatively high load occurs in steps, with the sizes of integer multiples measuring 2.7 nm. Since more than 10 myosin motors in an ensemble were involved in such sliding, their finding of stepwise displacement implies the presence of synchronous movement in ensemble myosin motors that generate the continuous sliding motion at a relatively high load. Their result together with the above considerations indicate that

when a continuous sliding movement exits between an actin filament and an ensemble of myosin motors, the motors are synchronized, regardless of whether the sliding filament is loaded or not.

Our finding begs the obvious question; What is the nature of the synchronization or cooperativity in the myosin actions producing the translational sliding movement of actin? There is some recent evidence suggesting a coordinated activity between the two heads of a myosin molecule[32,33]. However, the coordination between the two heads of a single myosin molecule does not lead to the length independence of D_m if individual myosin molecules with such double heads randomly interact with an actin filament. We performed a corresponding simulation with an additional assumption of a cooperative effect in the attachment between adjacent myosin heads, and obtained a 1/(actin length)-dependent D_m (see Supplementary Materials). Therefore, we believe that the cooperativity involved in the sliding movement generation is not between the two heads of a myosin molecule or among nearby myosin heads, but rather represents cooperativity between or among myosin heads some distance apart along an actin filament. Hancock & Howard[34] suggested the presence of a similar mechanical coordination between (or among) single-headed kinesin motors some distance apart along a sliding microtubule.

If we assume that myosins in an ensemble driving an actin filament to continuously slide act synchronously as if as a single mechanical unit, then the effective diffusion coefficient can be expected to be proportional to the average sliding velocity, since both are proportional to the frequency of the interaction of the single mechanical unit with a filament. This is what we found between the effective diffusion coefficient and the average sliding velocity (Fig. 5). Synchronization of ensemble myosin motors driving an actin filament to slide indicates that the sliding movement is not a property localized to the actions of individual myosin motors, but a property of the dynamical system consisting of ensemble motors and an actin filament. In this regard, it is interesting to note the report by Baker et al.[35] that the mechanochemical coupling of muscle contraction, the coupling of the force production by myosin motors with the chemical energy derived from the hydrolysis of ATP by the motors, is not localized to individual myosin heads in muscle.

It should be pointed out that the sliding speed of actin does not depend on the actin length (>~1 μm) (Fig. 4B). The length-independence of the velocity corresponds to the finding of Huxley & Julian[3] with muscle fibers shortening under a very light load, but does not provide any evidence that myosin is an independent force generator when generating unloaded (or light-loaded) sliding movement of actin, as is apparent from the fluctuation analysis shown in this work.

A similar length independence of D_m was previously found with microtubules sliding over kinesin or β-dynein *in vitro*, although kinesin or dynein heads were randomly oriented in these motility assays unlike in the present study[14,36]. The use of kinesin (or dynein) 'thick filaments' made of kinesin (or dynein) head-myosin rod chimera, from filaments whose projecting motors are supposed to be homogeneously oriented, is thus considered to be useful for confirming the length independence of D_m in these two cases.

In summary, myosin II motors in an ensemble generating the continuous sliding movement of an actin filament do not act independently, but rather cooperatively. Our finding thus indicates that understanding the mechanism of the sliding movement generated by myosin II requires the nonlinear collective dynamics of ensemble molecular motors rather than the linear average dynamics of single molecular motors[37].

Acknowledgments

We thank Drs. Ken Sekimoto and N. Thomas for valuable discussions, Dr. S. Chaen for help in the initial part of this work, Dr. K. Kinoshita for providing us with a Visual Basic version of the simulation program, and Dr. D. Falush for reading the manuscript. This work was supported by grants from the Ministry of Education, Science, Sports and Culture in Japan to KT, and in part by a grant from the Asahi Glass Foundation to KT.

References

1. Huxley, A. F. Review lecture: Muscular contraction. *J. Physiol.* (*Lond.*) **243**, 1–43 (1974).
2. Gordon, A. M., Huxley, A. F. & Julian, F. J. The variation in isometric tension with sarcomere length in vertebrate muscle fibers. *J. Physiol.* (*Lond.*) **184**, 170–192 (1966).
3. Huxley, A. F. & Julian, F. J. Speed of unloaded shortening in frog striated muscle fibers. *J. Physiol.* (*Lond.*) **177**, 60P–61P (1964).
4. van Kampen, N. G. *Stochastic Processes in Physics and Chemistry*, pp. 253–283 (North-Holland, Amsterdam, 1981).
5. Ishijima, A., Doi, T., Sakurada, K. & Yanagida, T. Sub-piconewton force fluctuation of actomyosin *in vitro*. *Nature* **352**, 301–306 (1991).
6. Kron, S. J. & Spudich, J. A. Fluorescent actin filaments move on myosin fixed to a glass surface. *Proc. Natl. Acad. Sci. USA* **83**, 6272–6276 (1986).
7. Sekimoto, K. & Tawada, K. Fluctuations in sliding motion generated by independent and random actions of protein motors. *Biophys. Chem.* **89**, 95–99 (2001).
8. Sekimoto, K. & Tawada, K. Extended time correlation of in vitro motility by motor protein. *Phys. Rev. Lett.* **75**, 180–183 (1995).
9. Yamada, A., Ishii, N. & Takahashi, K. Direction and speed of actin filaments moving over thick filaments isolated from molluscan smooth muscle. *J. Biochem.* **108**, 341–343 (1990).
10. Sellers, J. R. & Kachar, B. Polarity and velocity of sliding filaments: control of direction by actin and of speed by myosin. *Science* **249**, 406–408 (1990).
11. Spudich, J. A. & Watt, S. The regulation of rabbit skeletal muscle contraction. I. Biochemical studies of the interaction of the tropomyosin-troponin complex with actin and the proteolytic fragments of myosin. *J. Biol. Chem.* **246**, 4866–4871

(1971).
12. Yamada, A., Ishii, N., Shimmen, T. & Takahashi, K. MgATPase activity and motility of native thick filaments isolated from the anterior byssus retractor muscle of *Mytilus edulis*. *J. Muscle Res. Cell Motil.* **10**, 124–134 (1989).
13. Yamada, A. & Takahashi, K. Sudden increase in speed of an actin filament moving on myosin cross-bridges of 'mismatched' polarity observed when its leading end begins to interact with cross-bridges of 'matched' polarity. *J. Biochem.* **111**, 676–680 (1992).
14. Imafuku, Y., Toyoshima, Y. Y. & Tawada, K. Fluctuation in the microtubule sliding movement driven by kinesin *in vitro*. *Biophys. J.* **70**, 878–886 (1996).
15. Uyeda, T. P. Q., Warrick, H. M., Kron, S. J. & Spudich, J. A. Quantized velocities at low myosin densities in an *in vitro* motility assay. *Nature* **352**, 307–311 (1991).
16. Imafuku, Y., Toyoshima, Y. Y. & Tawada, K. Monte Carlo study for fluctuation analysis in the in vitro motility driven by protein motors. *Biophys. Chem.* **59**, 139–153 (1996).
17. Qian, H., Sheetz, M. P. & Elson, E. L. Single particle tracking. *Biophys. J.* **60**, 910–921 (1991).
18. Bevington, P. R., & Robinson, D. K. *Data Reduction and Error Analysis for the Physical Sciences*, 3rd ed., pp. 39–41 and pp. 197–200 (McGraw-Hill, Boston, 2003).
19. Tsaturyan, A. K., Koubassova, N., Ferenczi, M. A., Narayanan, T., Roessle, M. & Bershitsky, S. Strong binding of myosin heads stretches and twists the actin-helix. *Biophys. J.* **88**, 1902–1910 (2005).
20. Wakabayashi, K., Ueno, Y., Takezawa, Y. & Sugimoto, Y. Muscle contraction mechanism: use of synchrotron X-ray diffraction. *Encyclopedia of Life Sciences*, pp. 1–11 (Nature Publishing Group, London, 2001).
21. Bordas, J., Svensson, A., Rothery, M., Lowy, J., Diakun, G. P. & Boesecke, P. Extensibility and symmetry of actin filaments in contracting muscle. *Biophys. J.* **77**, 3197–3207 (1999).
22. Berg, H. C. *Random Walks in Biology*, pp. 48–64 (Princeton University Press, Princeton, 1993).
23. Vale, R. D., Soll, D. R. & Gibbons, I. R. One-dimensional diffusion of microtubules bound to flagellar dynein. *Cell* **5**, 915–925 (1989).
24. Chandra, R., Endow, S. A. & Salmon, E. D. An N-terminal truncation of the ncd motor protein supports diffusional movement of microtubules in motility assay. *J. Cell Sci.* **104**, 899–906 (1993).
25. Tawada, K. & Sekimoto, K. Protein friction exerted by motor enzymes through weak-binding interaction. *J. Theor. Biol.* **150**, 193–200 (1991).
26. Huxley, A. F. Muscle structure and theories of contraction. *Prog. Biophys. Biophys. Chem.* **7**, 255–318 (1957).
27. Takiguchi, K. & Higashi-Fujime, S. *In vitro* sliding movement of F-actin with HMM and S-1. *Cell Motil. Cytoskeleton* **10**, 347 (1988).
28. Toyoshima, Y. Y., Kron, S. J. & Spudich, J. A. Observation of in vitro movement of actin filament directed by myosin fragments bound to a nitrocellulose surface. *Cell Motil. Cytoskeleton* **10**, 347 (1988).
29. Uyeda, T. P. Q., Kron, S. J. & Spudich, J. A. Myosin step size. Estimation from slow sliding movement of actin over low densities of heavy meromyosin. *J. Mol. Biol.* **214**, 699–710 (1990).
30. Duke, T. A. J. Molecular model of muscle contraction. *Proc. Natl. Acad. Sci. USA* **96**, 2770–2775 (1999).
31. Liu, X. & Pollack, H. G. Stepwise sliding of single actin and myosin filaments. *Biophys. J.* **86**, 353–358 (2004).
32. Schoenberg, M. Cross-bridge head detachment rate constants determined from a model which explains the behavior of both weakly- and strongly-binding cross-bridges. *Adv. Exp. Med. Biol.* **453**, 425–434 (1998).
33. Tyska, M. J., Dupuis, D. E., Guilford, W. H., Patlak, J. B., Waller, G. S., Trybus, K. M., Warshaw, D. M. & Lowey, S. Two heads of myosin are better than one for generating force and motion. *Proc. Natl. Acad. Sci. USA* **96**, 4402–4407 (1999).
34. Hancock, W. O. & Howard, J. Processivity of the motor protein kinesin requires two heads. *J. Cell Biol.* **140**, 1395–1405 (1998).
35. Baker, J. E., LaConte, L. E. W., Brust-Mascher, I. & Thomas, D. D. Mechanochemical coupling in spin-labeled, active, isometric muscle. *Biophys. J.* **77**, 2657–2664 (1999).
36. Imafuku, Y., Toyoshima, Y. Y. & Tawada, K. Length dependence of displacement fluctuation and velocity in microtubule sliding movement driven by sea urchin sperm outer dynein *in vitro*. *Biophys. Chem.* **67**, 117–125 (1997).
37. Baker, J. E., Brosseau, C., Joel, P. B. & Warshaw, D. M. The biochemical kinetics underlying actin movement generated by one and many skeletal muscle myosin molecules. *Biophys. J.* **82**, 2134–2147 (2002).